Mo incorporation in MCM-41 type zeolite

Rohit Kumar Rana and B. Viswanathan *

Department of Chemistry, Indian Institute of Technology, Madras 600 036, India

Mo-incorporated MCM-41 has been prepared by direct hydrothermal synthesis. XRD and N_2-adsorption measurements showed the characteristics of MCM-41. IR, FT-Raman and UV-VIS DR spectroscopic analyses gave the evidences for the incorporation of Mo in the framework of MCM-41. They are found to be stable and active for cyclohexanol and cyclohexane oxidation reactions with H_2O_2 as oxidant. Activity of this system has been compared with that of Ti-MCM-41 and molybdena impregnated on pure siliceous MCM-41.

Keywords: metallosilicate, mesoporous, MCM-41, Mo-MCM-41, catalysis, oxidation

1. Introduction

Molecular sieves containing transition-metal ions in the framework positions exhibit remarkable properties as catalysts for a variety of oxidation reactions with peroxides as oxidant [1,2]. The potential of transition-metal-ion-containing zeolites is, however, limited because of the number and type of heteroelements that can be incorporated in the framework and also the pore sizes of the resulting molecular sieves.

Synthesis of molecular sieves by structure-directing effect of ordered aggregates of surfactant molecules [3] offers a means to obtain mesoporous molecular sieves with controlled pore sizes and with various heteroelements. Synthesis and characterization of MCM-41 containing Ti, V, Fe and Mn are reported in literature [4–7].

Molybdenum-containing catalysts are known to catalyze a variety of hydrogenation, oxidation and metathesis reactions [8–10]. Incorporation of Mo in the framework is limited because of the strain involved in the insertion of large transition-metal ions in the framework position. However, incorporation of Mo in the framework of MCM-41 is likely because of the greater flexibility of the structure as well as due to the differences in the mechanism of formation of these materials.

2. Experimental

2.1. Synthesis

MCM-41 and Mo-containing MCM-41 materials were synthesized under hydrothermal conditions at 388 K in a static stainless-steel autoclave. In a typical synthesis of Mo-MCM-41, to a 25% aqueous solution of cetyltrimethyl ammonium bromide (CTAB) (S.D. Fine Chem.) 4 g of 10% aqueous tetramethyl ammonium hydroxide (TMAOH) (S.D. Fine Chem.) was added. To this mixture 17.4 g of tetraethylorthosilicate (TEOS) (Merck) in ethanol and an aqueous solution of 0.2 g of sodium molybdate (S.D. Fine Chem.) were added simultaneously with vigorous stirring. The resulted gel was stirred for 1 h at room temperature. The typical molar gel composition was 1.0 SiO_2 : 0.01 MoO_3 : 0.23 CTAB : 60 H_2O. The gel was autoclaved at 388 K for 24 h. The solid product was filtered, washed several times with distilled water, dried in air at 373 K and, finally, calcined at 773 K for 8 h. In one of the preparations aluminium sulphate was added as the Al source to have both Al and Mo in the framework. Pure silica polymorph of MCM-41 was synthesized following the same procedure, except that no sodium molybdate was added. Mo contents of the resulted catalysts were analysed by spectrophotometric method [11]. Supported molybdena on MCM-41 (Mo-Im) was prepared by impregnation method taking ammonium molybdate as the Mo source and then calcining at 773 K for 5 h. Ti-MCM-41 was obtained by taking titaniumisopropoxide with H_2O_2 as the precursor for titanium and following the same procedure as that for Mo-MCM-41.

2.2. Characterization

All the samples have been characterized by X-ray diffraction (Rigaku miniflex, Fe-filtered Co-K_α radiation), IR spectroscopy (Shimadzu IR 470), FT-Raman spectroscopy (Bruker IFS 66v, YAG laser) and UV-VIS diffuse reflectance spectroscopy (Perkin Elmer, Lambda-14). Surface area and pore size measurements were carried out by N_2 adsorption on a Carlo Erba sorptometer (1800).

2.3. Catalytic activity

Oxidation of cyclohexanol was carried out at 328 K in a three-necked round bottomed flask under reflux conditions using 30 wt% H_2O_2 as oxidant and acetone as solvent. The temperature was maintained by a thermostated oil bath.

* To whom correspondence should be addressed.

For oxidation of cyclohexane, reaction was performed in a PARR (4842) autoclave at 423 K for 3 h. Quantitative analyses of the products were done by gas chromatography using a Nucon GC fitted with a FID. Turnover frequency (TF) was calculated as mmol of cyclohexane or cyclohexanol converted per mmol of active metal sites per unit reaction time in minutes. For cyclohexane oxidation, conversion values were corrected by subtracting the amount ($<1\%$ g/g) obtained for blank reaction. In the given reaction conditions (namely 328 K), oxidation of the solvent acetone was not detected for the reaction of cyclohexanol [12].

3. Results and discussion

3.1. XRD

Figure 1 illustrates the powder X-ray diffractograms of various samples prepared both by hydrothermal method and impregnation on MCM-41. The pattern may be indexed on the basis of hexagonal lattice characteristic of MCM-41 structure [3]. It is observed that in all the samples no phases corresponding to MoO_3 or molybdate species were present. Absence of MoO_3 or molybdate species even in the impregnated samples is probably due to the presence of X-ray insensitive amorphous phase. Kovacheva et al. [13] have reported the absence of such species on Mo-impregnated HY zeolite. The d_{100} values are given in table 1 along with corresponding unit cell parameters (a_0). No apparent changes in unit cell parameters are observed in the case of Mo-MCM-41. It may be inferred that most of the Mo are
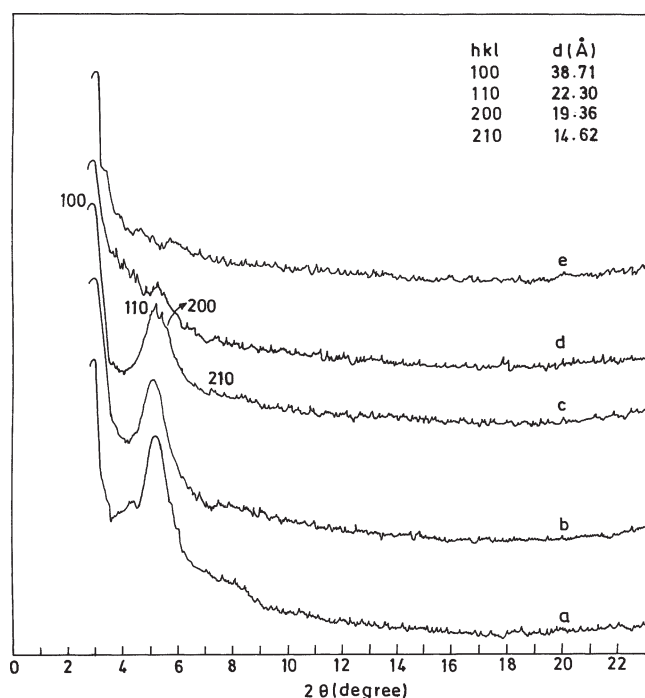
not incorporated into the framework position of MCM-41. Loss of crystallinity is observed for Mo-impregnated samples as the intensities of the higher angle peaks diminished. Chemical analysis of the calcined Mo-MCM-41 samples indicates not all of Mo present in the synthesis gel is incorporated into the framework. Weight percentages of Mo in the calcined Mo-MCM-41 were 0.05 and 0.1 in comparison to 0.28 and 0.46, respectively, in the gel for two different compositions.

3.2. N_2 adsorption

In order to evaluate the porosity of the materials, N_2 adsorption was carried out. Figure 2 shows the N_2-adsorption–desorption isotherm for Mo-MCM-41 with pore-size distribution curve (inset). For all samples, the isotherms are similar having inflection around $P/P_0 =$

Table 1
Structural and textural characteristics of systems.

Sample	d_{100} (Å)	a_0[a] (Å)	Pore size (Å)	FWT[b] (Å)	Pore volume (cm³/g)	S_{BET} (m²/g)
MCM-41	38.0	44.0	28	16.0	0.70	1032
Mo-MCM-41 (0.05)	38.5	44.5	27	17.5	0.67	982
Mo-MCM-41 (0.10)	38.7	44.7	26	18.7	0.66	948
Ti-MCM-41 (0.06)	39.4	45.5	27	18.5	0.65	974
Mo-Im (0.06)	38.0	44.0	23	21.0	0.42	706
Mo-Im (0.10)	38.3	44.2	23	21.2	0.46	608

[a] $a_0 = 2d_{100}/\sqrt{3}$.
[b] FWT: framework thickness $= a_0 -$ pore size.

hkl	d (Å)
100	38.71
110	22.30
200	19.36
210	14.62

Figure 1. XRD patterns for calcined samples of (a) siliceous MCM-41, (b) Mo-MCM-41 (0.05% MoO_3), (c) Mo-MCM-41 (0.10% MoO_3), (d) Mo-Im (0.10% MoO_3) and (e) Mo-Im (1.0% MoO_3).
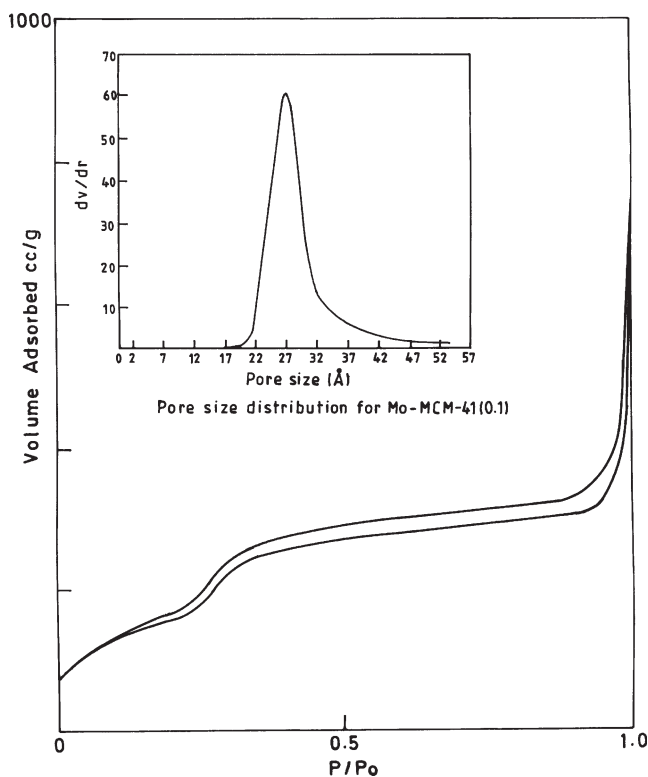

Figure 2. N_2-adsorption–desorption isotherm and pore-size distribution for Mo-MCM-41 (0.10% MoO_3).

0.20–0.30 characteristic of mesoporous materials with uniform pore size [3]. Surface area calculated by BJH method, average pore sizes and specific pore volume for the various samples are given in table 1. The decrease in surface area for the impregnated samples can be attributed to the loss in crystallinity seen in the XRD patterns. There was not appreciable variation in the pore sizes among Mo-MCM-41 and siliceous MCM-41 samples. Wall thickness calculated by subtracting pore diameter from a_0 unit cell parameter shows there is increase in thickness for metal-containing samples from that of pure siliceous MCM-41. This increase in wall thickness for Mo-MCM-41 is in the same range as reported by Zhang et al. [14] for Ti-MCM-41, where they have attributed this to the metal incorporation in the walls of the mesoporous silicate framework. Decrease in pore size and pore volume for the impregnated samples shows that the pore surface is covered by molybdenum species, which is further evident from the increase in wall thickness.

3.3. IR spectroscopy

The IR spectra of the samples show bands characteristic of the MCM-41 [3] (figure 3). A band around 963 cm^{-1} is observed for Mo-containing MCM-41. This is assigned to Si–O–Mo vibration present in the framework of MCM-41. Similar assignment has been made for Ti- and V-containing molecular sieves [15,16]. Klemperer et al. [17] have also assigned this band to Si–O–Mo vibration present in crystals of the type (R$_3$SiOMoO$_3$)[(C$_4$H$_9$)$_4$N], where R = C$_6$H$_5$ and t-C$_4$H$_9$. However, this cannot be taken as a proof

for metal incorporation in the case of MCM-41, because silanol groups present in pure siliceous MCM-41 give the same band [18]. The absorption band at 905 cm^{-1}, which is observed for impregnated samples only, can be assigned to Mo–O vibrations in tetrahedral molybdate species attached to the surface [17]. It is seen that this band is present in the impregnated samples (refer the inset in figure 3), while it is absent in the Mo-incorporated MCM-41. It is, therefore, deduced that the procedure adopted in this study could have resulted in the incorporation of Mo in the MCM-41 lattice. The ν_s(Si–O–Si) band, which decreases from 804 cm^{-1} in pure siliceous MCM-41 to 798 cm^{-1} in Mo-MCM-41 samples, is also another indication for the formation of Mo-incorporated MCM-41. This aspect has been considered by Alba et al. [19]. The band assignment for the infrared spectrum of Mo-MCM-41 is given in table 2. The apparent loss of crystallinity of the samples prepared by impregnation and the presence of the band around 905 cm^{-1} imply interaction of Mo with OH groups of MCM-41.

Table 2
Band assignments in IR spectra of Mo-MCM-41.

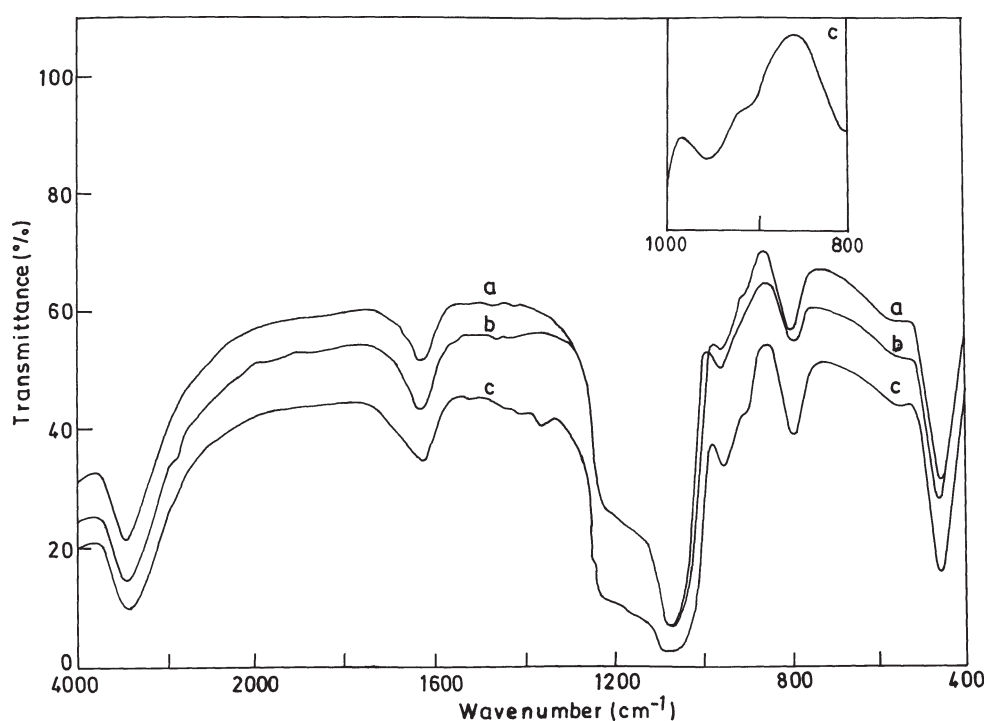| Wavenumber (cm^{-1})	Assignment
3440	ν_{OH}(Si–O–H)
1632	δ_{OH}(H$_2$O)
1232, 1081	ν_{as}(Si–O–Si)
963	ν_{as}(Si–O–Mo) or ν(Si–OH)
794, 544	ν_s(Si–O–Si)
460	δ(Si–O–Si)

Figure 3. Framework IR spectra for the calcined samples of (a) Mo-Im (0.10% MoO$_3$), (b) Mo-MCM-41 (0.10% MoO$_3$) and (c) Mo-Im (1.0% MoO$_3$). (Inset shows enlarged portion of the spectrum for sample (c) in the region 1000–800 cm^{-1}.)
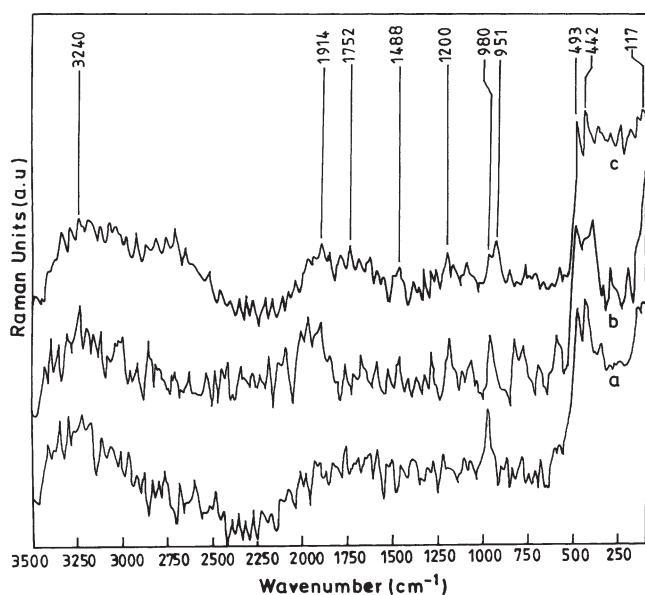
Figure 4. Ft-Raman spectra for calcined samples of (a) siliceous MCM-41, (b) Mo-Im (0.10% MoO_3) and (c) Mo-MCM-41 (0.10% MoO_3).

Figure 5. UV-VIS DR spectra for calcined samples of (a) Mo-MCM-41 (0.10% MoO_3), (b) Mo-Im (0.10% MoO_3) and (c) Mo-Im (1.0% MoO_3).

3.4. FT-Raman

Raman spectroscopy together with UV-VIS diffuse reflectance spectroscopy is widely used for the characterization of supported molybdena catalysts [20]. FT-Raman spectra of various samples are given in figure 4. Pure siliceous MCM-41 gives characteristic bands at 983, 493 (442) and 117 cm^{-1}. They are assigned to Si–OH, six- or four-membered ring vibrations and bending mode of Si–O–Si vibrations, respectively [21]. For Mo-MCM-41, a band around 951 cm^{-1} was observed. This is tentatively assigned to tetrahedral MoO_4^{2-} species present in the framework. As the quality of the Raman spectra is not very good, further analysis of the spectra is not attempted at present.

3.5. UV-VIS DRS

To obtain the coordination around Mo^{6+}, UV-VIS spectroscopy was applied in a diffuse reflectance mode. This is known to be a good technique for the characterization of transition-metal-incorporated zeolites [15,16]. UV-VIS DR spectra of various samples are shown in figure 5.

Various oxomolybdenum compounds give absorption bands in UV-VIS region due to ligand–metal charge transfer (O^{2-}–Mo^{6+}). The position of this electronic transition depends on the ligand field symmetry surrounding the Mo center. For oxygen ligands, a higher energy transition is expected for tetrahedral Mo^{6+} than for an octahedral one [22]. Traditionally, absorption bands from 250–280 nm have been assigned to $Mo(T_d)$, and bands from 300–330 nm were assigned to $Mo(O_h)$ [23].

Mo-MCM-41 gives two bands at 242 and 277 nm indicating the presence of two types of $Mo^{6+}(T_d)$ species. Whereas in the case of impregnated samples, bands were
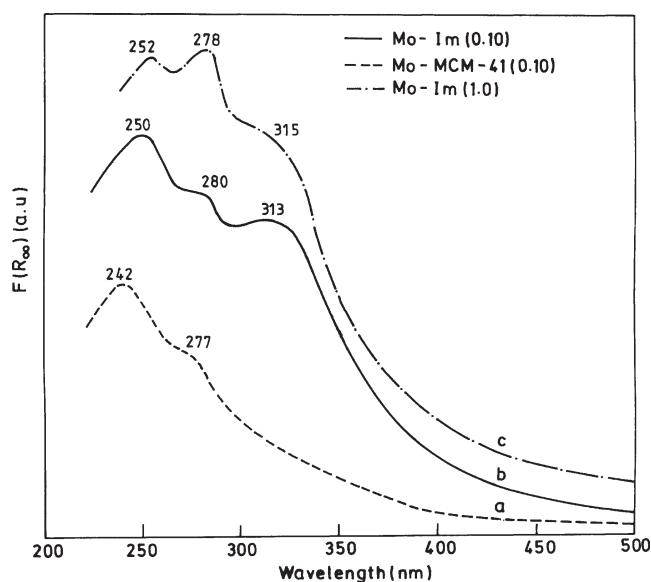
Table 3
Oxidation of cyclohexanol (acetone : cyclohexanol : H_2O_2 of 10 : 2 : 1 (v/v/v), 0.1 g of catalyst, 328 K, 5 h).

Catalyst	MoO_3 (wt%)	TF (min^{-1})
Mo-MCM-41	0.05	23
	0.10	24
Mo-Im	0.06	2
	0.10	3
Ti-MCM-41	0.06 (wt% TiO_2)	16
Al,Mo-MCM-41	0.08	17

obtained due to both tetrahedral and octahedral Mo^{6+} coordinations. Since with increase in condensation the band shifts towards higher wavelength [23], out of the two bands, the band at lower wavelength can be due to isolated MoO_4^{2-} species, and the other one at higher wavelength can be due to polymeric MoO_4^{2-} species. Comparison of the band at lower wavelength for Mo-MCM-41 and impregnated samples shows that there is a shift of 10 nm towards lower wavelength for Mo-MCM-41. This shift was attributed to Mo incorporation in the framework. Similar observations have been reported for Ti- and V-containing molecular sieves [15,16]. The band at 315 nm for impregnated samples indicates the presence of MoO_3 species [24].

3.6. Catalytic activity

The catalytic activity of the samples prepared was evaluated for cyclohexanol oxidation and cyclohexane oxidation reactions using 30 wt% H_2O_2. The TFs obtained for cyclohexanol oxidation on various catalysts are given in table 3.

Mo-MCM-41 prepared by hydrothermal method shows a higher turnover frequency in comparison with the samples prepared by impregnation method (Mo-Im). Higher disper-

Table 4
Oxidation of cyclohexane (acetone : cyclohexane : H_2O_2 of 15 : 2 : 1 (v/v/v), 0.1 g of catalyst, 432 K, 3 h).

Catalyst	MoO_3 (wt%)	TF (min^{-1})	Selectivity (mol%)	
			Cyclohexanol	Cyclohexanone
Mo-MCM-41	0.05	49	14.38	85.62
	0.10	53	12.41	87.59
Mo-Im	0.06	7	20.78	79.22
	0.10	11	21.41	78.59
Ti-MCM-41	0.06 (wt% TiO_2)	21	17.15	82.85
Al,Mo-MCM-41	0.08	28	18.50	81.50

sion and site isolation of the active center Mo in the case of Mo-MCM-41 catalysts can be attributed for enhanced activity. The activity is lowered with repeated cycles using the activated spent catalysts in the case of samples prepared by impregnation method, whereas it does not vary for Mo-MCM-41. The loss of activity may be due to the leaching of Mo from silica surface in oxygen-transfer reactions with H_2O_2 [25]. Ti-MCM-41 also shows appreciable activity for cyclohexanol oxidation reaction comparable to that of Mo-MCM-41 samples (cf. table 2). For the sample containing Al, the activity is found to be less than that of Mo-MCM-41. This is because of increase in the hydrophilicity due to presence of Al^{3+}, which hinders the approach of the organic substrate to the active site.

The data on the activity of the catalysts for cyclohexane oxidation are given in table 4. Similar trend analogous to cyclohexanol oxidation is observed in this case. It can be observed that the conversion for cyclohexane oxidation of Mo-MCM-41 is higher than that reported for TS-1 [26]. This is apparently because of the larger pore size of Mo-MCM-41 permitting a bulky molecule like cyclohexane into the pores in comparison to TS-1. Schuchardt et al. [26] have reported that the turnover numbers are in the range of 1–100 (TF < 1) for cyclohexane oxidation on TS-1 under comparable experimental conditions. The selectivity ratio of cyclohexanol to cyclohexanone is around 1 for TS-1, whereas it is in the order 0.15 for Mo-MCM-41, and is of the order 0.40 for the impregnated samples. It is seen that Mo-MCM-41 is more selective to the production of cyclohexanone.

4. Conclusions

Mo-MCM-41 samples prepared by hydrothermal synthesis are found to be crystalline with MCM-41 structure and have high surface area >900 m^2/g with pore diameter of 27 Å. Evidences for the presence of Mo in the framework were obtained from framework IR, FT-Raman and UV-VIS DR spectroscopic techniques. Mo-MCM-41 shows stable and higher activity for the oxidation of cyclohexanol and cyclohexane, in comparison to samples prepared by impregnation, due to the presence of Mo in the tetrahedral positions of the framework which results in site isolation of the active metal sites.

References

[1] B. Notari, Catal. Today 18 (1993) 163.
[2] P. Kumar, R. Kumar and B. Pandey, SYNLETT (1995) 289.
[3] J.S. Beck, J.C. Vartuli, W.J. Roth, M.E. Leonowicz, C.T. Kresge, K.D. Schmitt, C.T.-W. Chu, D.H. Olson, E.W. Sheppard, S.B. McCullen, J.B. Higgins and J.L. Schlenker, J. Am. Chem. Soc. 114 (1992) 10834.
[4] P.T. Tanev and T.J. Pinnavaia, Science 267 (1995) 865.
[5] K.M. Reddy, I. Moudrakovski and A. Sayari, J. Chem. Soc. Chem. Commun. (1994) 1059.
[6] Z.W. Yuan, S.Q. Liu, T.H. Chen, J.H. Wang and H.X. Li, J. Chem. Soc. Chem. Commun. (1995) 973.
[7] D. Zhao and D. Goldfarb, J. Chem. Soc. Chem. Commun. (1995) 875.
[8] E.A. Lombardo, M. Lo Jacono and W.K. Hall, J. Catal. 64 (1980) 50.
[9] G.W. Keulks, J. Catal. 19 (1970) 232.
[10] J.J. Rooney and A. Stewart, Spec. Period. Rep.: Catal. 1 (1977) 277.
[11] A.I. Vogel, *Text Book of Quantitative Inorganic Analysis*, 3rd Ed. (Longman, London, 1975) p. 903.
[12] W. Zhang, J. Wang, P.T. Tanev and T.J. Pinnavaia, J. Chem. Soc. Chem. Commun. (1996) 979.
[13] P. Kovacheva, N. Davidova and J. Novakova, Zeolites 11 (1991) 54.
[14] W. Zhang, M. Froba, J. Wang, P.T. Tanev, J. Wong and T.J. Pinnavaia, J. Am. Chem. Soc. 118 (1996) 9164.
[15] M.R. Boccuti, K.M. Rao, A. Zecchina, G. Leofanti and G. Petrini, in: *Structure and Reactivity of Surfaces*, Stud. Surf. Sci. Catal., Vol. 48, eds. C. Morterra, A. Zecchina and G. Costa (Elsevier, Amsterdam, 1989) p. 133.
[16] A. Thangaraj, R. Kumar and P. Ratnasamy, Appl. Catal. 57 (1990) L-1.
[17] W.G. Klemperer, V.V. Mainz, R.C. Wang and W. Shum, Inorg. Chem. 24 (1985) 1970.
[18] W. Kolodziejski, A. Corma, M.T. Navarro and J. Perez-Periente, J. Solid State Nucl. Magn. Reson. 2 (1993) 253.
[19] M.D. Alba, Z. Luan and J. Klinowski, J. Phys. Chem. 100 (1996) 2178.
[20] H. Jeziorowski and H. Knözinger, J. Phys. Chem. 83 (1979) 1166.
[21] P.K. Dutta and M. Puri, J. Phys. Chem. 91 (1987) 4329.
[22] F.A. Cotton and G. Wilkinson, *Advanced Inorganic Chemistry*, 4th Ed. (Wiley, New York, 1980) p. 847.
[23] M. Fournier, C. Louis, M. Che, P. Chaquin and D. Masure, J. Catal. 119 (1989) 400.
[24] C.C. Williams, J.G. Ekerdt, J.M. Jengh, F.D. Hardcastle, A.M. Turek and I.E. Wachs, J. Phys. Chem. 95 (1991) 8781.
[25] R.A. Sheldon, in: *Heterogeneous Catalysis and Fine Chemicals II*, Stud. Surf. Sci. Catal., Vol. 59, eds. M. Guisnet et al. (Elsevier, Amsterdam, 1991) p. 33.
[26] U. Schuchardt, H.O. Pastore and E.V. Spinace, in: *Zeolites and Related Microporous Materials: State of Art*, Stud. Surf. Sci. Catal., Vol. 84, eds. J. Weitkamp, H.G. Karge, H. Pfeifer and W. Hölderich (Elsevier, Amsterdam, 1994) p. 1877.